Observation of Gain in a Free-Electron-Laser Master Oscillator–Power Amplifier

L. Vintro,[1],[a] S. V. Benson,[1],[a] A. Bhowmik,[2] M. S. Curtin,[2] J. M. J. Madey,[1],[b] W. A. McMullin,[2] and B. A. Richman[1]

[1]*Stanford Photon Research Laboratory, Stanford University, Stanford, California 94305*

[2]*Rocketdyne Division, Rockwell International, 6633 Canoga Avenue, Canoga Park, California 91303*

(Received 29 August 1989)

We report the first operation of a master oscillatory–power amplifier in which both devices are free-electron lasers. Gain optimization in the power amplifier was studied. A 35-A electron beam produced up to 60% gain at 3 μm. The gain spectrum was obtained by gap tuning the power-amplifier wiggler and evidence was found for violation of the Madey theorem due to high-gain effects.

PACS numbers: 42.55.Tb, 52.60.+h

Results from the first operation of a free-electron-laser master oscillator–power amplifier (FEL-MOPA), in which both the master oscillator (MO) and the power amplifier (PA) are FEL's, are reported. Both the MO and PA are driven in succession by an electron beam from a radio-frequency linear accelerator (rf linac) with the same electrons contributing to gain in the MO and PA. The high electron-beam quality required in the PA is assured by operating the MO in the small-signal, unsaturated regime. Up to 60% gain has been observed at 3 μm in the PA with the parameters of Table I.

The optical components in an FEL oscillator are susceptible to intense laser radiation and harmonics produced by the FEL. The radiation often degrades[1] and damages the resonator optics. Thus, power scalability of an rf FEL oscillator is seriously limited by its optics. By adopting a MOPA configuration this constraint may be relaxed with an MO at moderate power followed by one or more high-power amplifier stages[2] to attain the desired power levels. An important advantage of the FEL, wavelength tunability, is thereby preserved. The purpose of the present experiment was to demonstrate the MOPA concept with an untapered PA operating in the small-signal gain regime. Gain optimization in the PA was studied through input mode matching, and transverse and axial overlap of the optical and electron pulses. At optimum matching conditions, the gain spectrum was obtained by gap tuning the PA wiggler. The gain spectrum is markedly different from that predicted by the low-gain Madey theorem.[3] The main features of the experiment are described below; a detailed description can be found elsewhere.[4,5]

The Mark III rf linac provides an electron beam with the parameters of Table I. The electron beam is first transported through the Mark III FEL[6] which serves as the MO. The wiggler in this device is a 47-period, planar, permanent magnet hybrid with a period of 2.3 cm. The wiggler is gap tunable and is operated at 4.5 kG. After leaving the MO, an electron beam line transports and matches the beam into the Rocketdyne wiggler[7] which serves as the PA. The PA uses a planar permanent magnet wiggler whose gap and field taper may be continuously tuned over the range given in Table I. A Brewster plate permits outcoupling of radiation from the MO resonator. The optical beam is transported to the PA with turning mirrors and is spatially matched and synchronized to the electron beam in the PA by a mode-matching telescope and an optical delay, respectively. The telescope permits variation of either the waist size or its position in the PA, while maintaining the other variable constant. The waist can be located at any point in the PA, and its radius can be varied by $\pm 10\%$. The delay is an optical trombone with a range of 10.5 cm. An

TABLE I. FEL-MOPA parameters.

Electron beam	
Peak current	35 A
Normalized emittance	
Vertical	2π mm mrad
Horizontal	10π mm mrad
Waist	
Vertical	0.3 mm
Horizontal	0.7 mm
Energy	38 MeV
Energy spread	0.5%
Macropulse length	3 μs
Micropulse length	3 ps
Input optical beam at power amplifier	
Wavelength	3 μm
Wavelength spread	0.6%
Macropulse length	2 μs
Micropulse length	2 ps
Waist	1 mm
Average energy	3 mJ
Peak power at small signal	100 kW
Power-amplifier wiggler	
Length	200 cm
Period	2.5 cm
Variable gap	0.76–2.0 cm
Peak magnetic field	3.7–0.8 kG

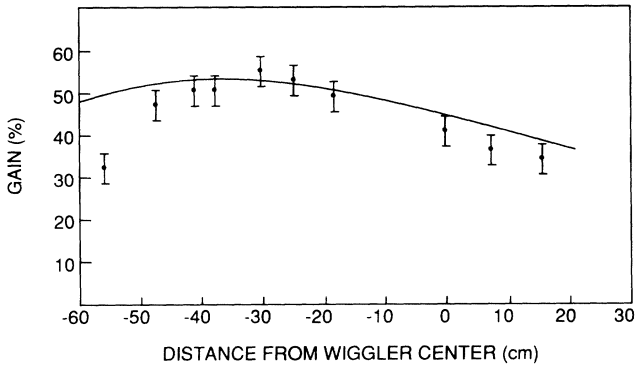

FIG. 1. Gain vs location of the optical waist. The electron waist is −30 cm from the wiggler center. Solid curve is FELEX simulation.

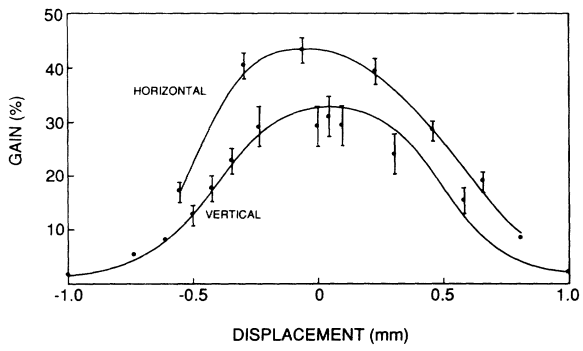

FIG. 3. Gain vs vertical and horizontal displacement between the optical and electron beams. Solid curves are FELEX simulations.

optical chopper with a fixed delay window provides a reference signal. Properties of the optical beam injected into the PA are summarized in Table I. The radiation emerging from the PA is transported to diagnostics, while the electron beam is sent to a beam dump. The reference and amplified signals are measured with high-speed Ge:Au detectors. The ratio of these signals gives a direct measure of amplification.

Conditions for optimum gain in the PA were studied. With the electron and optical pulses synchronized to each other, the effect of relative spatial location between the beam waists on the gain was examined. The electron waist was −30 cm (upstream) from the wiggler center. The optical waist radius was 1 mm and its location was scanned from −55 to 15 cm about the wiggler center. Results are shown in Fig. 1. Peak gain occurs where the waists overlap. The solid curve in Fig. 1 was obtained using the Los Alamos National Laboratory FEL simulation code FELEX[8] with the parameters of Table I, and assumes a square electron pulse shape and an initial Gaussian TEM_{00} optical mode. The simulation and data points are in good agreement. Similar results were obtained with the electron waist −40 cm from the wiggler center. In the latter case the peak gain was 40%, while for the former it was 55%.

The effect of axial displacement between the optical and electron pulses on gain was determined with the beam waists both −30 cm from the wiggler center. Using the optical delay, the optical pulse was moved relative to the electron pulse ±1 mm above the position where peak gain was observed. The result is depicted in Fig. 2. The solid curve in Fig. 2 was obtained using FELEX with a square electron pulse shape. Again good agreement between the simulation and data points was found. Also, a simulation with a Gaussian electron pulse shape was performed. The result with the square pulse gave a much better fit to the data, indicating the actual pulse shape is closely approximated by a square. The full width at half maximum (FWHM) of the curve in Fig. 2 is 0.8 mm, which corresponds to an electron micropulse length of 3 ps. The asymmetry in the gain versus delay curve is due to pulse slippage effects which are quite strong with such short microbunches.

Gain sensitivity to vertical and horizontal overlap of the optical and electron beams was also obtained. The location of the waists and axial displacement were set at values where optimum gain occurred. Using two of the turning mirrors, the optical beam was translated in the vertical plane at a fixed horizontal-plane location, and

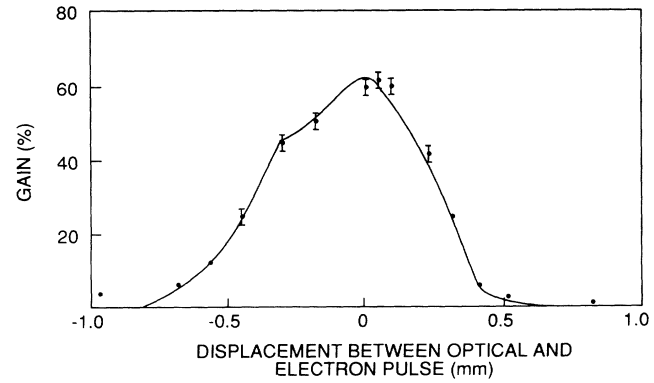

FIG. 2. Gain vs axial displacement between the optical and electron pulses. Solid curve is a FELEX simulation.

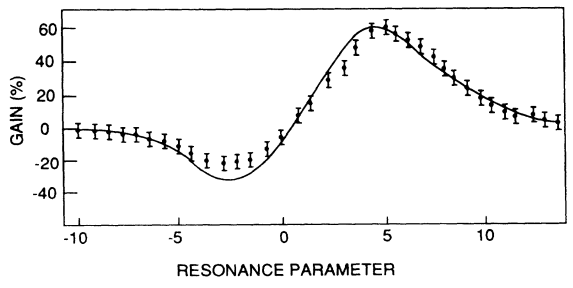

FIG. 4. Gain vs resonator parameter. Solid curve is a FELEX simulation.

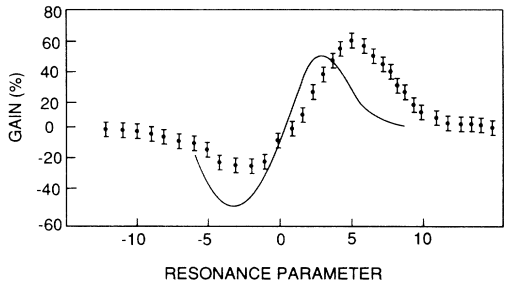

FIG. 5. Gain vs resonance parameter. Solid curve is the derivative of the forward spontaneous emission spectrum.

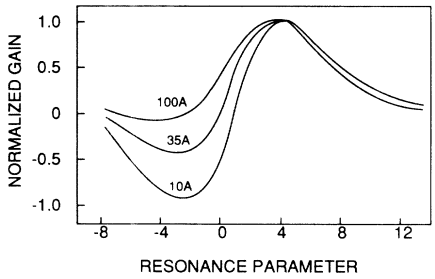

FIG. 6. FELEX simulations of normalized gain vs resonance parameter for peak currents of 10, 35, and 100 A and parameters of Table I.

vice versa, with the beams remaining parallel to one another. The vertical and horizontal scan range was ± 1 mm about the position where peak gain occurred. Gain as a function of vertical and horizontal displacement was obtained, with results shown in Fig. 3. For the vertical scan the FWHM of a FELEX simulation was 0.9 mm, while for the horizontal scan it was 1.2 mm.

The gain spectrum at optimum matching and overlap conditions was obtained by gap tuning the PA wiggler from 3.7 to 3.5 kG. The measured gain as a function of the resonance parameter is shown in Fig. 4. The resonance parameter v in Fig. 4 is defined by $v=[(k-k_0)\times v-\omega]L$, where k_0 is the wiggler wave number, L is the wiggler length, v is the electron axial velocity, and k and ω are the optical wave number and frequency. The solid curve is a FELEX simulation with the parameters of Table I. Excellent agreement between the simulation and data is seen in Fig. 4. The amplification peak of 60% occurs when v is 4.3, while the absorption peak of -35% occurs at -2.2.

In the low-gain limit, the gain is known to vary with resonance parameter as the derivative of the spontaneous power spectrum.[3,9] As shown in Fig. 5, the functional form of the gain measured in this experiment departs substantially from the derivative of the spontaneous spectrum. Although a number of factors may contribute to this discrepancy, we believe that the primary cause of this discrepancy is the onset of exponential gain characteristic of FEL operation in the high-gain regime.

Several authors[10-13] have demonstrated theoretically that the form of the spontaneous spectrum and gain line shapes in the low-gain regime should depend on the divergence of the optical mode into which the electron beam is made to radiate.

The effect has also been demonstrated experimentally by Deacon and Xie.[14] However, in all cases the integral of the gain line shape in the low-gain regime is identically equal to zero. The gain line shape measured in this experiment, whose integral is manifestly not equal to zero, can thus not be explained within the limits of the low-gain theory.

Two possible effects contribute to the asymmetry of the gain line shape in the intermediate- and high-gain regimes (see Fig. 6). In the high-gain limit, the exponential growth of the amplified modes will clearly yield an amplification factor $(P_{\text{out}}-P_{\text{in}})/P_{\text{in}}$ greater than the absorption due to the competing attenuated modes.

The input-mode-matching requirements also differ for the amplified and attenuated modes in the high-gain regime. As has been shown by several authors[15,16] the gain (or attenuation) in high-gain systems is optimized when the optical mode at the input to the undulator takes the form of the complex conjugate of the mode to be excited. Amplification is thus optimized when the waist of the input optical mode lies within the undulator, while attenuation is optimized when the waist is placed in front of the undulator. As the input mode matching in this experiment was adjusted to optimize the gain, significantly less power was coupled to the attenuated modes responsible for absorption.

Although we have not analyzed the relative contributions of exponential growth and input mode matching to the data shown in Figs. 4 and 5, the excellent agreement of the observed data with the numerical FELEX simulation provides persuasive evidence of the dominance of high-gain effects in this experiment.

In conclusion, an all-FEL MOPA has been operated for the first time in the small-signal, unsaturated regime with results in excellent agreement with computer simulations. Future experiments will be performed with an electro-optic switch in a modified Mark III FEL optical cavity. This will allow some of the electron micropulses to pass through the MO without lasing and enter the PA unperturbed. The electro-optic switch will also allow dumping of the MO optical cavity. In this configuration it will be possible to perform both small- and large-signal experiments with the Rocketdyne wiggler.

This work was supported by Los Alamos National Laboratory Contract No. 9-XFH1725G-1. Valuable contributions by the following individuals are gratefully acknowledged: B. Burdick, M. Emamian, J. Haydon, and E. Szarmes at Stanford University; J. Brown, E. Curtis, R. Hassler, P. Metty, and K. Widen at Rocketdyne; and D. A. G. Deacon at Deacon Research. We

thank B. McVey and M. Schmitt at Los Alamos National Laboratory for the FELEX calculations.

---

[a]Now at Wharton School of Business, University of Pennsylvania, Philadelphia, PA 19104.

[b]Now at Department of Physics, Duke University, Durham, NC 27706.

[1]D. A. G. Deacon, Nucl. Instrum. Methods Phys. Res., Sect. A **250**, 283 (1986), and references therein.

[2]A. Bhowmik, J. M. J. Madey, and S. V. Benson, Nucl. Instrum. Methods Phys. Res., Sect. A **272**, 183 (1988).

[3]J. M. J. Madey, Nuovo Cimento **50B**, 64 (1979).

[4]A. Bhowmik *et al.*, in Proceedings of the International Conference on Lasers '88, Lake Tahoe, Nevada, December 1988 (to be published).

[5]L. Vintro, Ph.D. dissertation, Stanford University, 1989 (unpublished).

[6]S. V. Benson *et al.*, Nucl. Instrum. Methods Phys. Res., Sect. A **250**, 39 (1986).

[7]A. Bhowmik *et al.*, Nucl. Instrum. Methods Phys. Res., Sect. A **272**, 10 (1988).

[8]B. D. McVey, Nucl. Instrum. Methods Phys. Res., Sect. A **250**, 449 (1986).

[9]N. M. Kroll, in *Physics of Quantum Electronics,* edited by S. F. Jacobs and M. Sargent (Addison-Wesley, Reading, MA, 1982), Vol. 8, p. 315.

[10]W. B. Colson and P. Elleaume, Appl. Phys. B **29**, 101 (1982).

[11]P. Luchini, G. Prisco, and S. Solimeno, Proc. SPIE **453**, 283 (1984).

[12]C. C. Shih, Proc. SPIE **453**, 205 (1984).

[13]W. B. Colson, in *Physics of Quantum Electronics,* edited by S. F. Jacobs and M. Sargent (Addison-Wesley, Reading, MA, 1982), Vol. 8, p. 457.

[14]D. A. G. Deacon and M. Xie, IEEE J. Quant. Electron. **21**, 939 (1985).

[15]G. T. Moore, Nucl. Instrum. Methods Phys. Res., Sect. A **239**, 381 (1985); **239**, 418 (1985).

[16]M. Xie, Ph.D. dissertation, Stanford University, 1988 (unpublished).